

# C-Terminal Fibronectin Exerts Beneficial Effects in Reducing Tissue Damage and Modulating Macrophage Function in a Murine Septic Model

Haili Geng, Yong Wu, Yuanzhong Chen

Fujian Institute of Hematology, Fujian Provincial Key Laboratory on Hematology, Fujian Medical University Union Hospital, Fuzhou, Fujian, 350001, People's Republic of China

Correspondence: Yuanzhong Chen, Fujian Institute of Hematology, Fujian Provincial Key Laboratory on Hematology, Fujian Medical University Union Hospital, No. 29 Xinquan Road, Fuzhou, Fujian, 350001, People's Republic of China, Tel +86-13306908368, Email chenyz@mail.fjmu.edu.cn; TP123123gtt@163.com

**Background:** Fibronectin (FN) can improve organ function and slow the progression of sepsis, but full-length FN is hard to be exacted as a therapeutic.

**Objective:** This study aimed to investigate the beneficial effects of C-terminal heparin-binding domain polypeptide of FN (rhFNHC-36) in a cecal ligation and puncture (CLP)-mediated murine septic model and explore its regulatory effects on macrophages.

**Methods:** Mice were randomly assigned to four groups: unoperated control (Normal), sham operation control (Sham), CLP-operation with intravenous injection of phosphate-buffered saline (CLP+PBS), and CLP-operation with rhFNHC-36 treatment (CLP+rhFNHC-36). Blood and abdominal fluid samples were subjected to bacterial colony formation assays. Organs (liver, spleen, and lung) were undergone histopathological analyses and/or weighed to obtain organ indices. Serum interleukin-6 (IL-6) levels, nitric oxide (NO) release from isolated abdominal macrophages, and chemotactic effect of macrophages were measured with commercial kits. Surface programmed death ligand 1 (PD-L1) expression on macrophages was measured by flow cytometry.

**Results:** Mice in the CLP+PBS group showed a lower survival rate than that in the CLP+rhFNHC-36 group. Improved survival was associated with better clearance of bacterial pathogens, as evidenced by colony formation assays. The CLP-induced decrease in thymus and spleen indices was attenuated by rhFNHC-36 treatments. rhFNHC-36 alleviated sepsis-associated tissue damage in liver, spleen, and lung. CLP-mediated increases in plasma IL-6 levels were reversed by rhFNHC-36 treatment. NO levels in peritoneal macrophages after lipopolysaccharides (LPS)-stimulation in the CLP+rhFNHC-36 group were lower than that in the CLP+PBS group. Notably, macrophages from the CLP+rhFNHC-36 group retained better chemotaxis ability. After LPS challenge, these macrophages had a reduced percentage of PD-L1-positive cells compared to those in the CLP+PBS group.

**Conclusion:** rhFNHC-36 improved survival of mice with CLP-induced sepsis by reducing tissue damage and modulating macrophage function. Our work provides critical insight for developing FN-based and macrophages-targeted therapeutics for treating sepsis.

**Keywords:** fibronectin, heparin-binding domain polypeptide, sepsis, macrophage, cecal ligation and puncture

## Introduction

Sepsis is a systemic inflammatory response against invading pathogenic bacteria and their toxins that usually causes severe tissue and organ damage.<sup>1,2</sup> Sepsis is considered a public health emergency, with a mortality rate of approximately 30–70%.<sup>3,4</sup> Sepsis was reported to be the leading cause of death globally in 2020 among immunocompromised individuals, including seniors, pregnant women, newborns and hospitalized individuals.<sup>5</sup> The pathogenesis of sepsis involves inflammation, immune and tissue damage, and pathophysiologic changes in multiple organs, resulting in disease complexity.<sup>1,2</sup> Notably, macrophages have been recognized to play essential roles in all phases of sepsis and affect both immune homeostasis and inflammatory processes. As such, macrophage dysfunction is considered a major cause of sepsis-induced immunosuppression.<sup>6,7</sup>

Mononuclear macrophages are important factors in the innate immune system, as they are the first line of defense against infection.<sup>8</sup> During severe trauma and infection, bacterial components such as endotoxins stimulate mononuclear macrophages to release excessive inflammatory cytokines such as tumor necrosis factor  $\alpha$  (TNF- $\alpha$ ), interleukin (IL)-10, and IL-6.<sup>9</sup> These cytokines can enhance the phagocytic ability of the macrophages and recruit antigen-presenting cells to trigger adaptive immunity by acting on the co-stimulatory molecule on the surface of T cells.<sup>10</sup> Many studies showed that macrophages isolated from septic patients or animals exhibited a state of unresponsiveness or response tolerance after lipopolysaccharides (LPS) stimulation *in vitro*. This was manifested by altered expression of some immune surface markers, such as an upregulation of the inhibitory co-stimulatory molecule programmed death ligand 1 (PD-L1),<sup>11–13</sup> as well as decreased phagocytic ability of macrophages.<sup>14–17</sup> All of these changes suggest that macrophage dysfunction leads to immune unresponsiveness in patients with sepsis. Macrophages also produce inducible nitric oxide synthase, which decomposes arginine, leading to the production and release of nitric oxide (NO).<sup>18</sup> NO is not only an important second messenger in cell signaling, but it also plays a significant role in immunomodulation.<sup>18</sup> NO is an effector molecule in the innate immune system and has an immune-regulatory effect in killing pathogenic microorganisms and tumor cells. However, excessive NO is cytotoxic.<sup>19</sup> As an important inflammatory mediator produced by activated macrophages, NO in excessive amounts usually reflects the severity of the inflammatory response during sepsis.<sup>19</sup>

Many studies have reported that fibronectin (FN) can be used to evaluate the severity of sepsis.<sup>20</sup> Supplements containing FN-rich cryoprecipitate have been shown to improve cardio-pulmonary function as well control the progression of sepsis.<sup>21</sup> In terms of diagnosis and prognosis, clinical improvement of patient outcomes correlates with an increase in plasma FN level, indicating its value as a biomarker of sepsis.<sup>22</sup> However, many studies have reported the difficulty of extracting FN in its high molecular weight (450 kDa) form from donor plasma. In addition, there is a potential risk of transmission of blood-borne diseases with extracting FN.<sup>23</sup> Therefore, it is necessary to explore the possibility of generating FN with only the functional domain using genetic engineering, which could lead to a safer and more effective treatment for sepsis. Previously, we successfully expressed and purified C-terminal heparin-binding domain of FN (rhFNHC-36) using a yeast expression system,<sup>24,25</sup> and reported that rhFNHC-36 alone could improve the survival of galactosamine-sensitized mice with endotoxemia and colibacillemia by preventing inflammatory responses.<sup>24,25</sup> However, whether rhFNHC-36 also exhibits beneficial effects in sepsis has not been intensively studied.

In this study, we established a murine model of sepsis using a cecal ligation and puncture (CLP) model, which approximates the clinical presentation of sepsis and is commonly used to study different pathological and physiological stages of sepsis.<sup>26</sup> Using the CLP mouse model, we evaluated the protective effects of rhFNHC-36 in bacterial clearance, organ atrophy, tissue damage, and dysregulated inflammation during sepsis. In addition, the mechanisms of action of rhFNHC-36 in modulating macrophage activities were explored.

## Materials and Methods

### Animals

Inbred male C57BL/6 mice (aged 8–10 weeks, weighing 20±2 g) were purchased from SLAC Laboratory Animal Co. Ltd (Shanghai, China). Mice were housed at the specific pathogen-free (SPF) facility at the Animal Center of Fujian Medical University at room temperature (22±1 °C) with a 12/12-hour light/dark cycle and access to food and water *ad libitum*. All animal experiments in this study were approved by the Institutional Animal Care and Use Committee of Fujian Medical University (Approval No. SCXK- 2012-0001). All animal experiments followed the Guide for the Care and Use of Laboratory Animals (2011 Eighth Edition, National Research Council) for the welfare of the laboratory animals.

### CLP-Induced Sepsis Animal Model

This study followed the standard protocol to induce acute sepsis in mice by cecal ligation and puncture, as described by Rittirsch et al.<sup>27</sup> All procedures were performed using aseptic technique. Mice were fasted the day prior to the operation. Each mouse was weighed and intraperitoneally injected with 1% pentobarbital (8 mL/kg body weight) for general anesthesia. The mouse was dissected along the linea alba (midlines white fascia) of the abdominal musculature, and an

intermuscular incision of approximately 1 cm was made. Subsequently, the cecum was located and ligated with a 4/0 silk thread. During cecal puncture, the cecum was perforated with an 18G needle, making a single through-and-through puncture midway between the ligations. A small droplet of feces was extruded from each of the mesenteric and antimesenteric penetration sites. After that, the cecum was placed back into the abdominal cavity, which was then closed with a 6/0 silk thread. A total of 1 mL of prewarmed (37 °C) 0.9% sterile normal saline solution was subcutaneously injected, and food and water were provided after the procedure.

## Study Design

Mice were randomly assigned to the following four groups (n=10 per group): unoperated control (Normal), sham operation control (Sham), phosphate-buffered saline (PBS) control (CLP+PBS), and rhFNHC-36 treatment group (CLP+rhFNHC-36). Mice in the Normal group were unoperated, while mice in the Sham group were dissected without CLP. In the CLP+PBS and CLP+rhFNHC-36 groups, mice underwent CLP, and PBS or rhFNHC-36 (Xiamen Amoytop Biotech Co., Ltd., Xiamen, China) at a dose of 40 mg/kg body weight was intravenously injected through the tail veins, respectively. The intravenous tail injection was performed at three time points: 0.5 h, 1 h, and 2 h after surgery.

## Bacterial Colony Formation Assays

Blood and abdominal fluid samples were collected from each mouse 6 h after the operation. Samples were diluted 100-fold and plated on blood agar dishes with rich solid medium, and the total number of bacterial populations was estimated by colony counts. Identification of bacterial isolates was performed using the Microgen GNA ID (MID) bacteria identification kit (Huan Kai, Guangdong, China).

## Hematoxylin and Eosin (H and E) Staining

Three mice were randomly selected from each group for histopathological analyses. At 24 h after CLP, mice were dissected and organ morphologies of the liver, spleen, and lung were observed. After isolation, organs (spleen and thymus) were weighed to obtain organ indices (organ weight in g per body weight of mouse in kg). After isolation, liver, spleen, and lung were washed and fixed in 10% formalin solution. Tissue samples were dehydrated with ethanol and Xylene, embedded in paraffin wax, and sectioned into 5-micron thin slices. After being affixed to a microscope slide (60–65°C for 1–2 h), samples were dewaxed with Xylene and washed with ethanol and water. The slides were first placed in hematoxylin staining solution for 7 min and then in eosin for 1 min. After washing with ethanol and water, the slides were mounted with xylene and imaged under a microscope.

## Enzyme-Linked Immunosorbent Assay (ELISA)

Blood samples were collected from each mouse via the orbital vein 6 h after the operation. Blood was anticoagulated with heparin sodium and centrifuged at 10,000 g for 10 min at 4°C. The supernatant was collected and diluted 75 times for subsequent ELISA analyses. The mouse IL-6 ELISA Kit (Millipore, USA) was used to measure the IL-6 levels following the manufacturer's protocol. Blank and standard wells were marked and duplicate wells were set up on an ELISA 96-well plate. All other wells were reserved for test samples. Optical measurements were analyzed using the optical absorption enzyme analyzer Sunrise<sup>TM</sup> (TECAN, Switzerland).

## Macrophage Isolation and Purity Evaluation

C57BL/6 mice were euthanatized by cervical dislocation 24 h after CLP. Each mouse was bathed in 75% ethanol for 30 s, fixed on a wax dissection tray. The animal was dissected along the midline of the abdominal skin with care to prevent tissue damage and contamination. Each mouse was injected with pre-cooled PBS intraperitoneally, followed by a gentle rub on the abdominal area for 2–5 min to harvest the macrophages in PBS. Macrophage-containing PBS was collected from the abdominal cavity and washed twice by centrifugation (400 g, 5 min). The cell count in each sample was obtained, and harvested macrophages were resuspended and diluted to  $2 \times 10^6$  cells/mL in Roswell Park Memorial Institute (RPMI)-1640 medium (GIBCO, USA). The cells were incubated in a 24-well cell culture plate in a CO<sub>2</sub> incubator (SHELLAB, USA) at 37°C with 5% CO<sub>2</sub> for 4–5 h until the cells fully adhered to the bottom of each well. The

supernatant and any suspended cells were discarded, and the remaining cells were washed twice in RPMI-1640 medium with care. To assess the purity of the harvested macrophages, the cells adhering to the well were digested by trypsin and immunostained with fluorescein isothiocyanate (FITC)-conjugated anti-mouse CD14 antibody (eBiosciences, USA), as described below.

## NO Measurement in Macrophages

The macrophage suspension was added into a 96-well plate (200  $\mu$ L per well), and incubated at 37 °C for 4–5 h until cells became fully adherent. The supernatant and any suspended cell were discarded. Wells were washed twice with RPMI-1640 medium and then filled with RPMI-1640 complete medium containing lipopolysaccharides (LPS, at a final concentration of 1  $\mu$ g/mL; Sigma, Germany) to activate the macrophages. Untreated cells were set as the negative control. Cells were incubated further for 18–24 h and the supernatant was harvested. Griess Reagent kit (G2930, Promega, USA) was used to determine NO release from macrophages following the manufacturer's instructions. Optical density values were read at 540 nm (OD<sub>540</sub>) using the optical absorption enzyme analyzer Sunrise<sup>TM</sup> (TECAN, Switzerland). NO concentration was calculated as per the formula generated from the standard curve.

## Chemotactic Effect Assessment

The modified Boyden Chamber method was used for chemotactic assessment, as previously described.<sup>28</sup> Abdominal macrophages were resuspended in RPMI-1640 medium supplemented with 0.1% bovine serum albumin (BSA) to  $1 \times 10^6$  cells/mL. Then, 600  $\mu$ L of RPMI-1640 medium with 20 ng/mL murine Monocyte Chemotactic Protein-1 (MCP-1, Peprotech, USA) was added into the lower Transwell chamber (Millipore, USA), and the well filled with 600  $\mu$ L of RPMI-1640 medium without MCP-1 was used as the negative control. Subsequently, 100  $\mu$ L of the abdominal macrophage suspension was added into the upper Transwell chamber. The plate was incubated at 37 °C for 3 h. The residual cell suspension in the upper chamber was then discarded. To remove any non-migrating cells from the upper chamber, the membrane was cleaned with sterile cotton swabs, and the chamber was washed three times with 37 °C PBS. Each well was stained with 100  $\mu$ L of 0.25% crystal violet for 10 min. The chamber was washed 3–5 times with double distilled water and left to air dry. Samples were visualized under the Olympus IMT-2 inverted microscope (Pharmacia, USA). Five microscopic fields were randomly selected in each chamber and migrating macrophages on the lower surface of the chambers were counted. Chemotactic results are expressed as the chemotactic index (CI) under high power field of vision (200 $\times$ ). CI was calculated as the ratio of the number of macrophages migrating to the solution with the chemotactic factor to the number of those migrating to the control solution without the chemotactic factor.

## Flow Cytometry

After obtaining the macrophages, the corresponding fluorescein conjugated antibodies of the surface molecules to be labeled were added into the sample cell suspension. Cells were incubated for 15 min at 4 °C in the dark. CD14 (FITC anti-mouse CD14; eBiosciences, USA) and PD-L1 (Phycoerythrin (PE) anti-mouse PD-L1, BioLegend, USA) antibodies were used for analysis. Unbound antibodies were washed away by PBS. The precipitates were resuspended in 300  $\mu$ L of flow fixative for subsequent analyses. A flow cytometer (FACSVerse; BD Biosciences, USA) was used to measure PD-L1 expression on the surface of macrophages. Isotype and single-labeled controls of the fluorescein conjugated antibodies were used to calibrate the flow cytometer and calculate the percent of CD14-positive or PD-L1-positive cells.

## Statistics

Data are presented as mean  $\pm$  standard deviation (SD) and analyzed using SPSS 16.0 software (IBM, USA) and GraphPad Prism 5. 0 (GraphPad Software, USA) with a one-way analysis of variance (ANOVA). The survival rate of septic mice was evaluated using Kaplan-Meier via the Log rank test. A *P*-value less than 0.05 was considered statistically significant.

## Results

### rhFNHC-36 Improved the Survival of Mice with CLP-Induced Sepsis by Promoting Bacterial Clearance

We first evaluated the beneficial effect of rhFNHC-36 on the survival of septic mice following CLP-challenge. As shown in Figure 1A, mice in the CLP+rhFNHC-36 group had a reduced death rate compared to mice in the CLP+PBS group. No death was reported in the normal and sham operation groups. Death occurred on Day 2 after CLP in the CLP+PBS group and on Day 3 after CLP in the rhFNHC-36-treated group (CLP+rhFNHC-36). On Day 14 after surgery, the survival rate was only 50% in the CLP+PBS group, while the survival rate was 70% in the CLP + rhFNHC-36 group; the survival rate between these two groups was significant ( $P<0.05$ ).

To further investigate the mechanism underlying the survival benefit of rhFNHC-36, we compared the bacterial count in the blood and abdomen fluid samples of a representative mouse from each of the four groups. As shown in Figure 1B, no bacterial colonies in the blood or abdomen samples were observed in the normal group or sham operation group. Bacterial colony counts in the CLP+rhFNHC-36 group were significantly ( $P<0.01$ ) fewer than that in the CLP+PBS

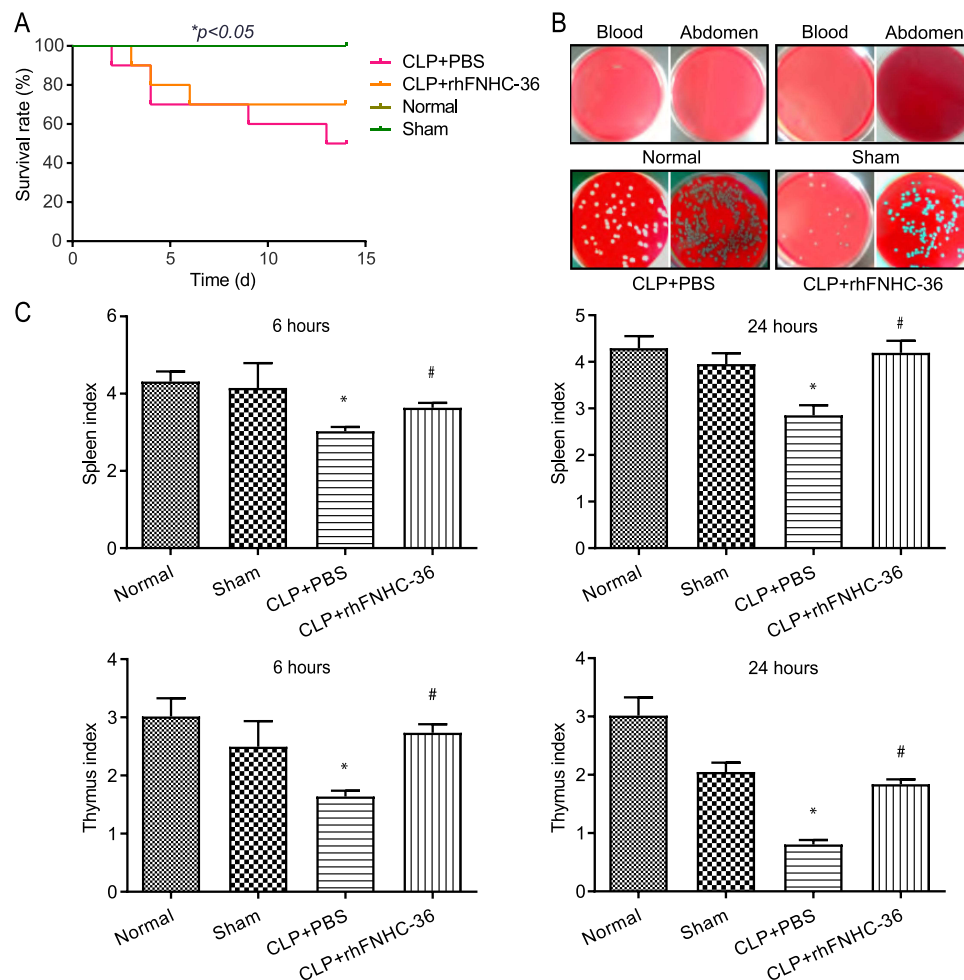


**Figure 1** rhFNHC-36 exerted beneficial effects on survival, promoted infection clearance rates, and reduced organ atrophy in mice with CLP-induced sepsis. **(A)** rhFNHC-36 decreased mortality of mice with CLP-induced sepsis. Survival rates were compared across all groups of mice during the period of 14 days after CLP. **(B)** Representative images of agar dishes show the bacterial colony growth for blood (left) or abdomen (right) samples from the indicated four groups. **(C)** Spleen and thymus indices were compared across the four groups at 6 h (left) and 24 h (right) after CLP, respectively.  $n=10$  for each group; \* $P<0.05$ , compared to the sham operation group; #  $P<0.05$  compared to the CLP+PBS group. Normal, mice were unoperated; Sham, mice were dissected without CLP; CLP+PBS, mice underwent CLP and were intravenously injected with PBS; CLP+rhFNHC-36, mice underwent CLP and were intravenously injected with rhFNHC-36.



group, for both samples from blood ( $1.4 \times 10^3 \pm 2.1 \times 10^2/\text{mL}$  vs  $3.4 \times 10^4 \pm 3.9 \times 10^3/\text{mL}$ ) and abdomen ( $4.0 \times 10^3 \pm 3.3 \times 10^3/\text{mL}$  vs  $3.9 \times 10^4 \pm 1.0 \times 10^4/\text{mL}$ ). Thus, rhFNHC-36 improved the survival of septic mice by aiding in the clearance of bacterial pathogens.

## rhFNHC-36 Relieved Organ Atrophy in Thymus and Spleen in CLP-Operated Septic Mice

We next examined the beneficial effects of rhFNHC-36 on organ atrophy by evaluating organ indices in the thymus and spleen at 6 h and 24 h after CLP (Table 1). We found that the thymus and spleen indices were not different between normal and sham mice. However, CLP-operated mice had lower thymus and spleen indices, suggesting the operation successfully induced organ atrophy during sepsis-induction. Spleen and thymus indices of septic mice increased markedly after rhFNHC-36 treatment, and the disease phenotype in terms of organ atrophy was partially rescued (Figure 1C and Table 1). Specifically, in the CLP+PBS group, the spleen index at 6 h and 24 h after operation was  $3.0 \pm 0.4$  and  $2.9 \pm 0.5$ , respectively; while in the CLP+rhFNHC-36 group, these indices were  $3.6 \pm 0.5$  and  $4.2 \pm 0.6$ , respectively. A similar increase in thymus index was also found in the CLP+rhFNHC-36 group at 6 h ( $1.6 \pm 0.3$  vs  $2.7 \pm 0.5$ ) and 24 h ( $0.8 \pm 0.2$  vs  $1.8 \pm 0.2$ ) after operation. It is worth noting that although rhFNHC-36 did not completely reverse the disease phenotype, there were significant differences in these indices between the two sepsis groups with and without rhFNHC-36 treatment.

## rhFNHC-36 Alleviated Tissue Damage in Liver, Spleen, and Lung in CLP-Operated Septic Mice

At 24 h after CLP operation, we examined the histopathology of the liver, spleen, and lung in all three groups. In the CLP+PBS group, there was extensive hemorrhaging, destruction of the hepatic lobule structure, widening of hepatic cord structures, and extensive hydropic degeneration of hepatocytes in the liver (Figure 2A), suggesting possible atrophy/apoptosis/necrosis of hepatocytes and congestion of liver sinuses. We also observed infiltration of inflammatory cells, including macrophages and lymphocytes, in the interstitium. In contrast, the rhFNHC-36-treated septic mice (CLP+rhFNHC-36) had less liver hemorrhage and congestion, as well as reduced degeneration and necrosis of hepatocytes with clear hepatic cord structures and full hepatocytes. There was also less infiltration of inflammatory cells in the CLP+rhFNHC-36 group, compared to the CLP+PBS group (Figure 2A).

Similarly, rhFNHC-36 alleviated disease phenotypes in the spleen (Figure 2B). Extensive hemorrhage was identified in the spleens of mice in the CLP+PBS group, with obvious atrophy of cortical lymphoid nodules, dilation of the medullary area, congestion of splenic sinuses, and increased inflammatory cell infiltration. However, mice in the CLP+rhFNHC-36 group only showed slight atrophy of lymphoid nodules, relieved congestion, and reduced infiltration of inflammatory cells.

**Table 1** Comparisons of Spleen and Thymus Indices at 6 h and 24 h After CLP in Mice

Group		Number of Mice	Spleen Index (mg/g)	Thymus Index mg/g)
6 h after CLP	Normal	10	$4.3 \pm 0.8$	$3.0 \pm 0.9$
	Sham	10	$4.1 \pm 1.4$	$2.5 \pm 1.1$
	CLP+PBS	10	$3.0 \pm 0.4$	$1.6 \pm 0.3$
	CLP+rhFNHC-36	10	$3.6 \pm 0.5$	$2.7 \pm 0.5$
24 h after CLP	Normal	10	$4.3 \pm 0.8$	$3.0 \pm 0.9$
	Sham	10	$4.0 \pm 0.5$	$2.0 \pm 0.3$
	CLP+PBS	10	$2.9 \pm 0.5$	$0.8 \pm 0.2$
	CLP+rhFNHC-36	10	$4.2 \pm 0.6$	$1.8 \pm 0.2$

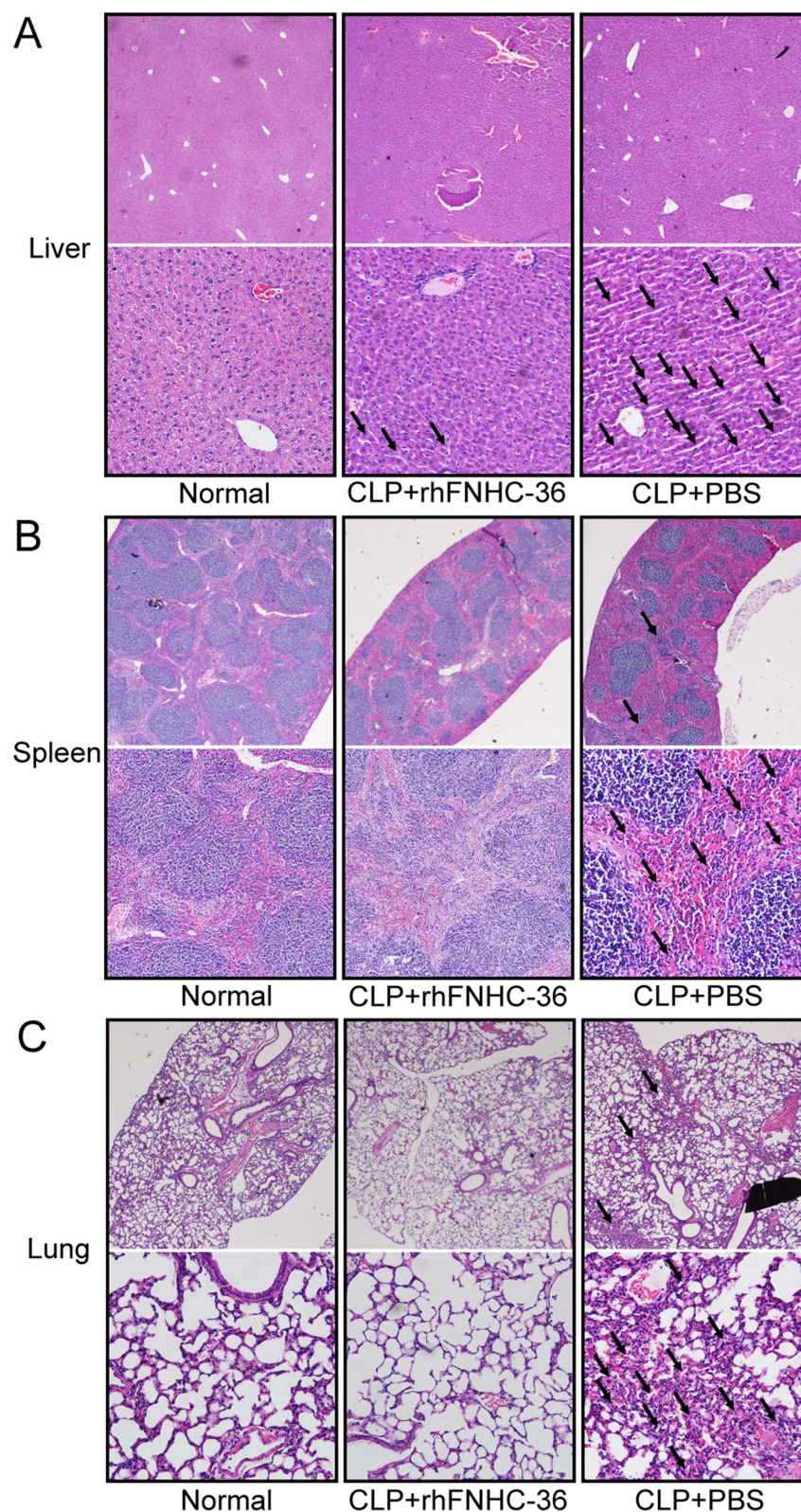


**Figure 2** rhFNHC-36 improved histological pathology in the liver, spleen, and lung tissues from mice with CLP-induced sepsis. **(A–C)** Representative images of H and E staining for liver **(A)**, spleen **(B)**, and lung **(C)** tissues of mice in the indicated groups. Each panel shows one tissue type sampled from the normal, CLP+rhFNHC-36 and CLP+ PBS groups, as indicated, at 24 h after CLP. Magnification: 100 $\times$ , upper panel; 400 $\times$ , lower panel. Arrows indicate the histopathologic changes in liver (compromised liver architecture and cellular integrity), spleen (disrupted structure of white pulp and red pulp, less apparent marginal zones), and lung (disrupted histological architecture, diffuse thickening in interstitial tissue with eosinophilic and histiocytic infiltration) tissues.

rhFNHC-36 also relieved the symptoms of atrophy in the lung (Figure 2C). Mice in the CLP+PBS group showed congestion of lung bronchi, obvious destruction of the alveolar septum, and inflammatory cell infiltration in the interspace. In contrast, rhFNHC-36 treatment resulted in less congestion of bronchi, clear alveolar septum structures, and decreased infiltration of inflammatory cells.

### rhFNHC-36 Suppressed Inflammation in Mice with CLP-Induced Sepsis

IL-6 is a pro-inflammatory cytokine produced at the site of inflammation, making it a reliable indicator of inflammation.<sup>29</sup> To assess the level of inflammation in septic mice, we quantitated plasma levels of IL-6 6 h after CLP operation (Figure 3). IL-6 levels were  $6.3 \pm 6.3$  pg/mL in the normal group and  $181 \pm 42$  pg/mL in the sham operation group. CLP operation significantly elevated plasma level of IL-6, reaching  $64,000 \pm 29,000$  pg/mL in the CLP+PBS group, suggesting extensive inflammatory responses were triggered by the injury. Upon treatment with rhFNHC-36, mice in the CLP+rhFNHC-36 group showed a significant decrease in plasma IL-6 levels ( $19,000 \pm 19,000$  pg/mL), compared to mice in the CLP+PBS group.

NO plays an important role in the cytostatic or cytotoxic activity of macrophages.<sup>30</sup> LPS was used to activate peritoneal macrophages isolated from mice in all 4 groups, and the concentration of NO produced by macrophages was measured to evaluate the effect of rhFNHC-36 in countering infection (Figure 4). Normal mice and sham mice had similar NO concentrations of  $4.2 \pm 1.6$   $\mu$ mol/L and  $4.6 \pm 1.1$   $\mu$ mol/L, respectively; while mice in the CLP+PBS group showed a significantly higher

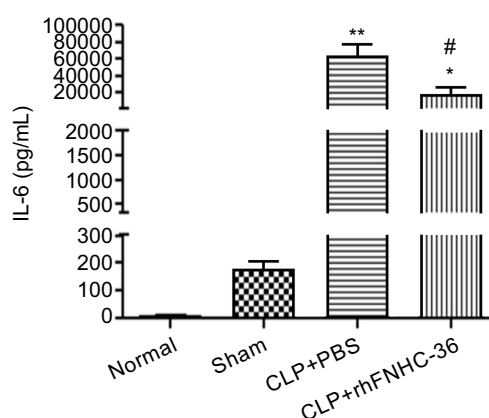


**Figure 3** rhFNHC-36 reduced plasma IL-6 levels in mice with CLP-induced sepsis. Plasma levels of IL-6 (pg/mL) in mice of the indicated four groups at 6 h after CLP were measured by ELISA.  $n=10$  for each group; \*  $P<0.05$ , \*\* $P<0.01$ , compared to the Sham group; # $P<0.05$ , compared to the CLP+PBS group.

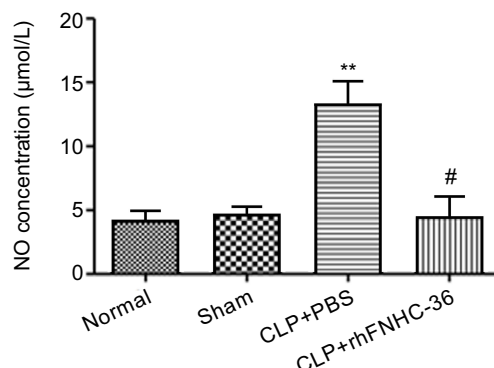


**Figure 4** rhFNHC-36 reduced NO production from peritoneal macrophages isolated from mice with CLP-induced sepsis. Peritoneal macrophages were isolated from mice of the indicated groups at 14 days after CLP. Following LPS (1  $\mu$ g/mL) stimulation of the isolated macrophages, NO production ( $\mu$ mol/L) was measured as an index of macrophage activation.  $n=10$  for each group; \*\* $P<0.01$ , compared to the sham operation group; #  $P<0.01$ , compared to the CLP+PBS group.



NO concentration ( $13.4 \pm 3.3 \mu\text{mol/L}$ ). Notably, mice in the CLP+rhFNHC-36 group demonstrated a NO concentration similar to those of normal and sham mice, which was reduced back to  $4.4 \pm 3.2 \mu\text{mol/L}$ . Therefore, rhFNHC-36 treatment was able to significantly reduce NO production and subsequently help control sepsis-related inflammation.

### rhFNHC-36 Promoted the Chemotaxis of Macrophages in Mice with Sepsis

Aside from their roles in chronic inflammation, macrophages also circulate in the blood to patrol for cell damage and infection.<sup>31</sup> rhFNHC-36 was shown to suppress inflammation in macrophages, but whether rhFNHC-36 disrupted the normal function of macrophages in terms of chemotaxis was unknown. Thus, we evaluated the migration of peritoneal macrophages by quantitating the CI. Compared to the normal group, both the CLP+PBS and CLP+rhFNHC-36 groups had a significant increase in CI after LPS stimulation (Figure 5A). However, the CI of the peritoneal macrophages in the CLP+rhFNHC-36 group was significantly higher ( $P < 0.05$ ) than that in the CLP+PBS group (Figure 5B). Therefore, rhFNHC-36 facilitated macrophage chemotaxis in our sepsis model.

### rhFNHC-36 Reduced the Percentage of PD-L1-Expressing Macrophages

Next, we investigated the mechanism by which rhFNHC-36 modulates macrophage activity. Upregulation of PD-L1 could result in macrophage death, subsequently compromising their function.<sup>32</sup> Thus, we evaluated the expression of PD-L1 on peritoneal macrophages upon LPS challenge using flow cytometry (Figure 6A). The percentage of PD-L1 positive cells in the LPS-induced peritoneal macrophages was  $69.0 \pm 10.9\%$  in normal mice and  $91.5 \pm 3.2\%$  in mice of the CLP+PBS group (Figure 6B). However, PD-L1 expression significantly decreased ( $80.4 \pm 3.9\%$ ) in the CLP+rhFNHC-36 group compared to the CLP+PBS group (Figure 6B). These results indicate that LPS stimulation increased PD-L1 expression in peritoneal macrophages, and that rhFNHC-36 treatment significantly attenuated the LPS-induced PD-L1 expression. Therefore, rhFNHC-36 may regulate macrophage activity possibly by lowering PD-L1 expression in septic mice.

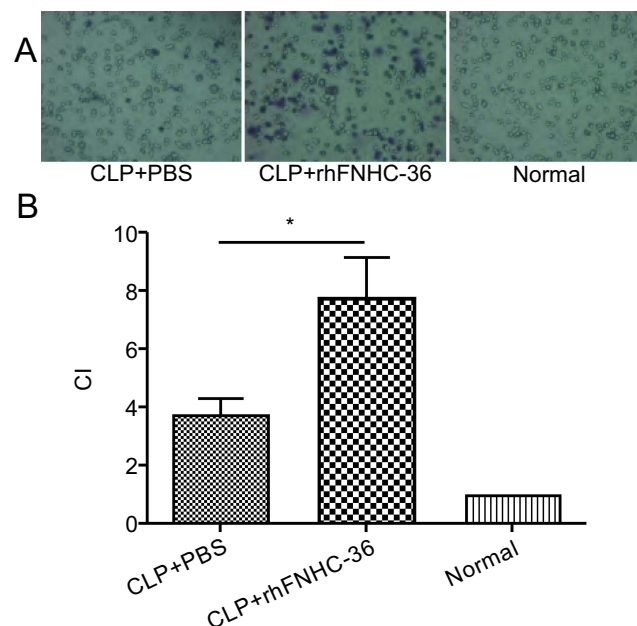


**Figure 5** rhFNHC-36 enhanced the chemotactic effects of peritoneal macrophages isolated from CLP-induced septic mice. **(A)** Representative microscopic images show the migration of peritoneal macrophages in the CLP+PBS, CLP+rhFNHC-36, and normal groups after LPS stimulation in the chemotactic effect assessment assays. Magnification, 40 $\times$ . **(B)** The chemotactic indices (CI) among the normal group and the indicated septic groups with PBS or rhFNHC-36 treatment.  $n=10$  for each group; \* $P < 0.05$ , compared to the CLP+PBS group.

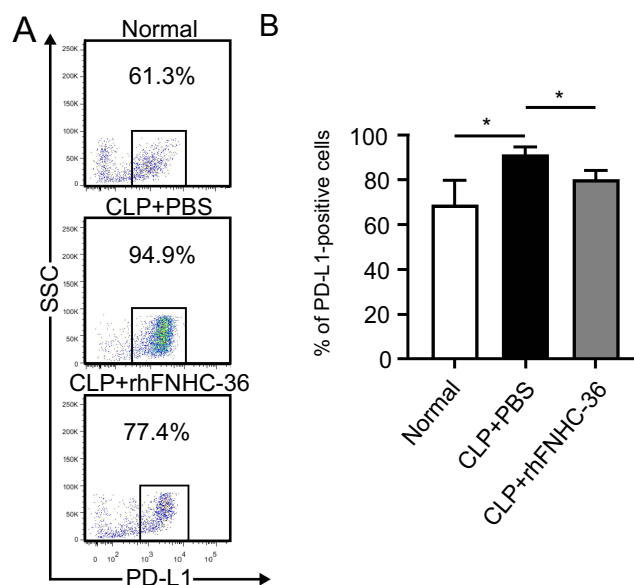


**Figure 6** rhFNHC-36 downregulated the percentage of PD-L1-positive cells in peritoneal macrophages isolated from CLP-induced septic mice. **(A-B)** Following LPS (1  $\mu$ g/mL) stimulation of the isolated macrophages for 18 h, the expression of inhibitory ligand PD-L1 on macrophages was evaluated using flow cytometry. Representative flow profiles of PD-L1 expression on LPS-stimulated macrophages in the indicated groups are shown **(A)**, and the percentages of PD-L1<sup>+</sup> population are summarized **(B)**.  $n=3$  for each group; \* $P < 0.05$ , between the indicated groups.

## Discussion

Sepsis is a dysregulated host response to the invasion of pathogenic bacteria and their toxins. Owing to its high incidence, mortality, and complex pathogenesis, sepsis is still a major challenge for public health globally.<sup>33</sup> Many studies have shown that fibronectin, a multi-functional glycoprotein, has an anti-sepsis effect.<sup>20–22,34</sup> However, no purified full-length FN agent has been used in clinical practice to date, partially because the heterologous expression of the FN molecule by gene recombination technology poses technical difficulties due to its large molecular weight. In this study, we evaluated the efficacy of the functional domain FN (rhFNHC-36) in a CLP-induced sepsis mouse model. We reported that rhFNHC-36 improved survival of septic mice and aided in the eradication of bacteria in the blood and abdomen. rhFNHC-36 also alleviated tissue atrophy of the liver, spleen, and lung. Moreover, we measured biomarkers, including IL-6 and NO production, chemotactic effects, and PD-L1 expression of macrophages, as indices of inflammation and macrophage function after rhFNHC-36 treatment. We found that rhFNHC-36 could improve outcomes in septic mice by limiting inflammation and regulating macrophage activity.

Sepsis results from an imbalance of inflammatory and anti-inflammatory responses.<sup>35</sup> Macrophages play a key role in the early defense against infection as a part of the innate immunity. Peritoneal macrophages help to maintain balance and stability of the body by ingesting foreign matter and apoptotic cells through phagocytosis.<sup>36</sup> These macrophages bind to the pathogenic microorganisms that are attached to the antibodies and complement factors. Macrophages phagocytize bacteria and work with the intracellular oxygen-dependent bactericidal system and proteolytic enzymes to digest, degrade, and eliminate pathogenic microbes out of the body.<sup>37–39</sup> On the other hand, macrophages also produce a wide range of molecules that participate in both the beneficial and detrimental aspects of inflammation, allowing these immune cells to become effective therapeutic targets of sepsis.<sup>6,7,40,41</sup> As shown in this study, rhFNHC-36 was able to govern the host inflammatory responses by regulating macrophage function. Maintaining the beneficial role of macrophages contributed to the effects of rhFNHC-36 in inhibiting aggressive systemic inflammation.

NO is produced by activated macrophages, giving them cytotoxic effects against invading pathogens and tumor cells. However, excessive NO may cause additional tissue damage.<sup>19</sup> In sepsis, NO can reflect the severity of the inflammatory response.<sup>19,42,43</sup> In this study, we found that peritoneal macrophages isolated from rhFNHC-36-treated septic mice produced less NO upon LPS challenge than the PBS-treated septic mice. This suggests that rhFNHC-36 protected septic mice from tissue

damage possibly via reducing the cytotoxic levels of NO. rhFNHC-36 also suppressed inflammatory responses by down-regulating IL-6 production in the serum. These results suggest that rhFNHC-36 can suppress inflammation through interacting with macrophages.

As an important indicator of the severity and prognosis of sepsis, IL-6 can be secreted from multiple cell types including fibroblasts, keratinocytes, mesangial cells, vascular endothelial cells, mast cells, macrophages, dendritic cells, and T and B cells.<sup>29,44</sup> Thus, whether the role of rhFNHC-36 in modulating other cell types also contributed to the downregulated production of IL-6 remains to be further explored, and other effector cytokines secreted by macrophages should not be overlooked. For example, the chemotactic effect of macrophages describes their ability to migrate to infection or lesion sites, which involves interactions between chemoattractant cytokines (chemokines) and macrophages.<sup>45</sup> We showed that after rhFNHC-36 treatment, macrophages were still able to maintain their basic function to migrate and patrol for infection. Therefore, it is plausible that rhFNHC-36 could enhance the chemotactic effect of macrophages, thus effectively preventing secondary infection in patients with sepsis.

Lastly, we speculated a possible mechanism by which rhFNHC-36 could regulate the macrophage function. Clinical studies showed that PD-L1, an apoptotic ligand expressed on the surface of mononuclear macrophages, plays an important role in reversing immune paralysis in patients with sepsis.<sup>12,13,46</sup> Upregulation of PD-L1 expression leads to cell death of macrophages and weakens host immunity, while the suppression of PD-L1 improves the survival rate of patients with sepsis and mitigates hepatocyte damage in patients with sepsis.<sup>12,13,46</sup> We are the first to report that rhFNHC-36 can downregulate PD-L1 expression in macrophages, and the beneficial effect of PD-L1 inhibition in our murine CLP model is consistent with previous clinical findings.

Previously, we showed that the expression of PD-1 on CD4<sup>+</sup> T cells increased after mice were challenged with LPS.<sup>24,25</sup> Subsequently, the inability of T cells to be activated during an infection resulted in immune paralysis in mice with sepsis.<sup>24,25</sup> In this study, flow cytometry analysis demonstrated increased PD-L1 expression on the surface of peritoneal macrophages isolated from mice with sepsis, which is consistent with our previous findings. However, rhFNHC-36 intervention downregulated PD-L1, which could aid in T-cell activation by suppressing the PD-1/PD-L1 immunoinhibitory axis and help attenuate the immune paralysis in septic mice. Therefore, rhFNHC-36 plays a protective role in sepsis by suppressing the expression of PD-L1 on the surface of macrophages. Further studies are needed to investigate the specific interaction between PD-L1 and rhFNHC-36.

In conclusion, we showed that rhFNHC-36 improved survival of mice with CLP-induced sepsis by reducing tissue damage and reversing immune paralysis. Our findings indicate that the beneficial effects of rhFNHC-36 are possibly attributed to its regulation on macrophage function. Taken together, we showed that macrophages could be an ideal therapeutic target to restrain aggressive inflammation in sepsis, and that utilizing the functional domain of FN, rhFNHC-36, could be a promising strategy for patients with sepsis. Our work highlights new insights into developing FN-based and macrophages-targeted therapeutics for treating sepsis.

## Abbreviations

FN, fibronectin; rhFNHC-36, C-terminal heparin-binding domain polypeptide of FN; CLP, cecal ligation and puncture; LPS, lipopolysaccharide; PD-L1, programmed death ligand 1; TNF- $\alpha$ , tumor necrosis factor  $\alpha$ ; IL, interleukin; NO, nitric oxide; MID, Microgen GNA ID; ELISA, Enzyme-linked immunosorbent assay; H and E, Hematoxylin and Eosin; BSA, bovine serum albumin; CI, chemotactic index; PE, Phycoerythrin; SPF, specific pathogen-free; SD, standard deviation; FITC, fluorescein isothiocyanate; PBS, Phosphate-buffered saline; RPMI, Roswell Park Memorial Institute; ANOVA, one-way analysis of variance.

## Data Sharing Statement

The data that support the findings of this study are available from the corresponding author upon reasonable request.

## Ethics Approval and Informed Consent

All animal experiments in this study were approved by the Institutional Animal Care and Use Committee of Fujian Medical University (Approval No. SCXK- 2012-0001). All animal experiments followed the Guide for the Care and

Use of Laboratory Animals (2011 Eighth Edition, National Research Council) for the welfare of the laboratory animals.

## Acknowledgments

We thank Medjaden Inc. for scientific editing of this manuscript.

## Author Contributions

All authors made a significant contribution to the work reported, whether that is in the conception, study design, execution, acquisition of data, analysis and interpretation, or in all these areas; took part in drafting, revising or critically reviewing the article; gave final approval of the version to be published; have agreed on the journal to which the article has been submitted; and agree to be accountable for all aspects of the work.

## Funding

This work was financially supported by the Grant/Award from the Investment Project of Fujian Provincial Development (No. 2060404), Overall Project of Fujian Medical University Union Hospital (No. 2015TC-1-004), Construction Project of Fujian Medical Center of Hematology (No. Min201704), National and Fujian Provincial Key Clinical Specialty Discipline Construction Program, P. R. C., and Science and Technology Innovation Joint Fund Project of Fujian Province (No. 2018Y9062).

## Disclosure

The authors declare that they have no known competing financial interests or personal relationships that could have appeared to influence the work reported in this paper.

## References

1. van der Poll T, van de Veerdonk FL, Scicluna BP, Netea MG. The immunopathology of sepsis and potential therapeutic targets. *Nat Rev Immunol.* **2017**;17:407–420. doi:10.1038/nri.2017.36
2. Huang M, Cai S, Su J. The Pathogenesis of Sepsis and Potential Therapeutic Targets. *Int J Mol Sci.* **2019**;20. doi:10.3390/ijms20215376
3. Balk RA. Optimum treatment of severe sepsis and septic shock: evidence in support of the recommendations. *Dis Mon.* **2004**;50:168–213. doi:10.1016/j.disamonth.2003.12.003
4. Fleischmann C, Scherag A, Adhikari NK, et al. Assessment of global incidence and mortality of hospital-treated sepsis. current estimates and limitations. *Am J Respir Crit Care Med.* **2016**;193:259–272. doi:10.1164/rccm.201504-0781OC
5. Rudd KE, Johnson SC, Agesa KM, et al. Global, regional, and national sepsis incidence and mortality, 1990–2017: analysis for the Global Burden of Disease Study. *Lancet.* **2020**;395:200–211. doi:10.1016/s0140-6736(19)
6. Chen X, Liu Y, Gao Y, Shou S, Chai Y. The roles of macrophage polarization in the host immune response to sepsis. *Int Immunopharmacol.* **2021**;96:107791. doi:10.1016/j.intimp.2021.107791
7. Cheng Y, Marion TN, Cao X, Wang W, Cao Y, Park 7: a Novel Therapeutic Target for Macrophages in Sepsis-Induced Immunosuppression. *Front Immunol.* **2018**;9:2632. doi:10.3389/fimmu.2018.02632
8. Wynn TA, Chawla A, Pollard JW. Macrophage biology in development, homeostasis and disease. *Nature.* **2013**;496:445–455. doi:10.1038/nature12034
9. Schulte W, Bernhagen J, Bucala R. Cytokines in sepsis: potent immunoregulators and potential therapeutic targets—an updated view. *Mediators Inflamm.* **2013**;2013:165974. doi:10.1155/2013/165974
10. Locati M, Curtale G, Mantovani A. Diversity, Mechanisms, and Significance of Macrophage Plasticity. *Annu Rev Pathol.* **2020**;15:123–147. doi:10.1146/annurev-pathmechdis-012418-012718
11. Zhu W, Bao R, Fan X, et al. PD-L1 blockade attenuated sepsis-induced liver injury in a mouse cecal ligation and puncture model. *Mediators Inflamm.* **2013**;2013:361501. doi:10.1155/2013/361501
12. Kyriazopoulou E, Giamarellos-Bourboulis EJ. Monitoring immunomodulation in patients with sepsis. *Expert Rev Mol Diagn.* **2021**;21:17–29. doi:10.1080/14737159.2020.1851199
13. Sari MI, Ilyas S. The Expression Levels and Concentrations of PD-1 and PD-L1 Proteins in Septic Patients: a Systematic Review. *Diagnostics.* **2022**;12. doi:10.3390/diagnostics12082004
14. Okano M, Azuma M, Yoshino T, et al. Differential role of CD80 and CD86 molecules in the induction and the effector phases of allergic rhinitis in mice. *Am J Respir Crit Care Med.* **2001**;164:1501–1507. doi:10.1164/ajrccm.164.8.2011072
15. Flohé SB, Agrawal H, Flohé S, Rani M, Bangen JM, Schade FU. Diversity of interferon gamma and granulocyte-macrophage colony-stimulating factor in restoring immune dysfunction of dendritic cells and macrophages during polymicrobial sepsis. *Mol Med.* **2008**;14:247–256. doi:10.2119/2007-00120.Flohe
16. Yan X, Tu H, Liu Y, Chen T, Cao J. Interleukin-17D Aggravates Sepsis by Inhibiting Macrophage Phagocytosis. *Crit Care Med.* **2020**;48:e58–e65. doi:10.1097/CCM.00000000000004070



17. Miao J, Ye P, Lan J, et al. Paeonol promotes the phagocytic ability of macrophages through confining HMGB1 to the nucleus. *Int Immunopharmacol*. 2020;89:107068. doi:10.1016/j.intimp.2020.107068
18. Bogdan C. Nitric oxide and the immune response. *Nat Immunol*. 2001;2:907–916. doi:10.1038/ni1001-907
19. Winkler MS, Kluge S, Holzmann M, et al. Markers of nitric oxide are associated with sepsis severity: an observational study. *Crit Care*. 2017;21:189. doi:10.1186/s13054-017-1782-2
20. Ruiz Martín G, Prieto Prieto J, Veiga de Cabo J, et al. Plasma fibronectin as a marker of sepsis. *Int J Infect Dis*. 2004;8:236–243. doi:10.1016/j.ijid.2003.10.005
21. Stevens LE, Clemmer TP, Laub RM, Miya F, Robbins L. Fibronectin in severe sepsis. *Surg Gynecol Obstet*. 1986;162:222–228.
22. Mamani M, Hashemi SH, Hajilooi M, Saedi F, Niayesh A, Fallah M. Evaluation of fibronectin and C-reactive protein levels in patients with sepsis: a case-control study. *Acta Med Iran*. 2012;50:404–410.
23. Yang F, Zhang Y, Cui X, et al. Extraction of Cell-Free Whole Blood Plasma Using a Dielectrophoresis-Based Microfluidic Device. *Biotechnol J*. 2019;14:e1800181. doi:10.1002/biot.201800181
24. Wu Y, Chen YZ, Huang HF, Chen P. Recombinant fibronectin polypeptide antagonizes hepatic failure induced by endotoxin in mice. *Acta Pharmacol Sin*. 2004;25:783–788.
25. Wu LQ, Yong WY, Zhang T, et al. C-terminal heparin-binding domain polypeptide derived from plasma fibronectin, rhFNHC36, protects endotoxemia mice by preventing inflammatory responses and increasing the activity of Th lymphocytes. *Int J Clin Exp Pathol*. 2017;10:6453–6461.
26. DeJager L, Pinheiro I, Dejonckheere E, Libert C. Cecal ligation and puncture: the gold standard model for polymicrobial sepsis? *Trends Microbiol*. 2011;19:198–208. doi:10.1016/j.tim.2011.01.001
27. Rittirsch D, Huber-Lang MS, Flierl MA, Ward PA. Immunodesign of experimental sepsis by cecal ligation and puncture. *Nat Protoc*. 2009;4:31–36. doi:10.1038/nprot.2008.214
28. Ott TR, Pahuja A, Lio FM, et al. A high-throughput chemotaxis assay for pharmacological characterization of chemokine receptors: utilization of U937 monocytic cells. *J Pharmacol Toxicol Methods*. 2005;51:105–114. doi:10.1016/j.vascn.2004.10.001
29. Tanaka T, Narazaki M, Kishimoto T. IL-6 in inflammation, immunity, and disease. *Cold Spring Harb Perspect Biol*. 2014;6:a016295. doi:10.1101/cshperspect.a016295
30. MacMicking J, Xie QW, Nathan C. Nitric oxide and macrophage function. *Annu Rev Immunol*. 1997;15:323–350. doi:10.1146/annurev.immunol.15.1.323
31. Shi C, Pamer EG. Monocyte recruitment during infection and inflammation. *Nat Rev Immunol*. 2011;11:762–774. doi:10.1038/nri3070
32. Nakamori Y, Park EJ, Shimaoka M. Immune Deregulation in Sepsis and Septic Shock: reversing Immune Paralysis by Targeting PD-1/PD-L1 Pathway. *Front Immunol*. 2020;11:624279. doi:10.3389/fimmu.2020.624279
33. Hunt A. Sepsis: an overview of the signs, symptoms, diagnosis, treatment and pathophysiology. *Emerg Nurse*. 2019;27:32–41. doi:10.7748/en.2019.e1926
34. Dellinger RP, Levy MM, Rhodes A, et al. Surviving Sepsis Campaign: international guidelines for management of severe sepsis and septic shock, 2012. *Intensive Care Med*. 2013;39:165–228. doi:10.1007/s00134-012-2769-8
35. von Dessauer B, Bongain J, Molina V, Quilodrán J, Castillo R, Rodrigo R. Oxidative stress as a novel target in pediatric sepsis management. *J Crit Care*. 2011;26:103.e101–107. doi:10.1016/j.jcrc.2010.05.001
36. Cassado Ados A, D'império lima MR, Bortoluci KR. Revisiting mouse peritoneal macrophages: heterogeneity, development, and function. *Front Immunol*. 2015;6:225. doi:10.3389/fimmu.2015.00225
37. Murray HW, Juangbhanich CW, Nathan CF, Cohn ZA. Macrophage oxygen-dependent antimicrobial activity. II. The role of oxygen intermediates. *J Exp Med*. 1979;150:950–964. doi:10.1084/jem.150.4.950
38. Qiu P, Liu Y, Zhang J. Review: the Role and Mechanisms of Macrophage Autophagy in Sepsis. *Inflammation*. 2019;42:6–19. doi:10.1007/s10753-018-0890-8
39. Weiss G, Schaible UE. Macrophage defense mechanisms against intracellular bacteria. *Immunol Rev*. 2015;264:182–203. doi:10.1111/imr.12266
40. Fujiwara N, Kobayashi K. Macrophages in inflammation. *Curr Drug Targets Inflamm Allergy*. 2005;4:281–286. doi:10.2174/1568010054022024
41. Kumar V. Targeting macrophage immunometabolism: dawn in the darkness of sepsis. *Int Immunopharmacol*. 2018;58:173–185. doi:10.1016/j.intimp.2018.03.005
42. Evans T, Carpenter A, Kinderman H, Cohen J. Evidence of increased nitric oxide production in patients with the sepsis syndrome. *Circ Shock*. 1993;41:77–81.
43. Lambden S. Bench to bedside review: therapeutic modulation of nitric oxide in sepsis—an update. *Intensive Care Med Exp*. 2019;7:64. doi:10.1186/s40635-019-0274-x
44. Velazquez-Salinas L, Verdugo-Rodriguez A, Rodriguez LL, Borca MV. The Role of Interleukin 6 During Viral Infections. *Front Microbiol*. 2019;10:1057. doi:10.3389/fmicb.2019.01057
45. Ruytinx P, Proost P, Van Damme J, Struyf S. Chemokine-Induced Macrophage Polarization in Inflammatory Conditions. *Front Immunol*. 2018;9:1930. doi:10.3389/fimmu.2018.01930
46. Chen R, Zhou L. PD-1 signaling pathway in sepsis: does it have a future? *Clin Immunol*. 2021;229:108742. doi:10.1016/j.clim.2021.108742